**RAA 2016** Vol. **16** No. **9**, 145 (6pp) doi: 10.1088/1674–4527/16/9/145
*http://www.raa-journal.org* *http://iopscience.iop.org/raa*

*Research in Astronomy and Astrophysics*

# Acoustic streaming and Sun's meridional circulation

Jose Manuel Valverde

Faculty of Physics, University of Seville, Avenida Reina Mercedes, 41012 Seville, Spain; *jmillan@us.es*

Received 2016 April 12; accepted 2016 May 20

**Abstract** A vast number of physical processes involving oscillations of a bounded viscous fluid are relevantly influenced by acoustic streaming. When this happens a steady circulation of fluid develops in a thin boundary adjacent to the interface. Some examples are refracted sound waves, a fluid inside a spherical cavity undergoing torsional oscillations or a pulsating liquid droplet. Steady streaming around circular interfaces consists of a hemispherically symmetric recirculation of fluid from the equatorial plane to the polar axes closely resembling the meridional circulation pattern observed in the Sun's convection zone that determines the solar cycle. In this paper, it is argued that the acoustic pulsations exhibited by the Sun would lead to acoustic streaming in the boundary of the convection zone. A simple estimation using a typical dominant frequency of 3 mHz and the observed surface oscillation amplitude yields a steady streaming velocity $u_\mathrm{s} \sim 10$ m s$^{-1}$, which is on the order of the meridional circulation velocity observed in the Sun's convection zone.

**Key words:** Sun: general — Sun: helioseismology — Sun: granulation — Sun: oscillations — Sun: fundamental parameters — Sun: activity

## 1 INTRODUCTION

The search for a correlation between steady meridional circulation (MC) currents in the convection zone (CZ) of the Sun and the solar activity cycle is a matter of great current interest (Arkhypov et al. 2012; Roudier et al. 2014; Hanasoge et al. 2015). Experimental evidence and simulations agree on the existence of a steady poleward MC in the near-surface layers of the Sun across both the northern and southern hemispheres with a characteristic velocity 10–20 m s$^{-1}$, which is superposed on the granular ($\sim$1 Mm across) and supergranular ($\sim$30–35 Mm across) convective cells (Hathaway 2011; Miesch & Hindman 2011; Featherstone & Miesch 2015; Hanasoge et al. 2015). The mean MC plays a central role in dynamo models and may largely regulate properties of the solar cycles (Choudhuri et al. 1995; Karak et al. 2014). Thus, determining the mechanisms that drive the MC as well as its main properties is of considerable interest. However, the structure of the MC in the deep CZ is a matter of active discussion. Observational studies yield controversial results on the equatorward flow required by mass conservation (Featherstone & Miesch 2015).

Early studies based on SOHO/MDI suggested that the MC would span at least the upper half of the CZ, whose base is determined to be at $r = 0.713R_\odot$, where $R_\odot = 6.96 \times 10^8$ m is the Sun's radius. Thus, the double-cell MC pattern employed by different models to predict the solar activity cycle usually assumes a deep return flow at depths below $r = 0.85R_\odot$ (Pipin & Kosovichev 2013; Hazra et al. 2014; Lord et al. 2014). Yet, more recent helioseismic investigations indicate that a return equatorward flow would occur at shallower depths ($r \sim 0.95R_\odot$) with perhaps other meridional cells stacked beneath the one nearest the surface (Hathaway 2011; Miesch & Hindman 2011; Hanasoge et al. 2015). A rotational boundary layer would take place entirely within a sharply stratified shear layer at the upper edge of the solar convective envelope ($0.95R_\odot < r < R_\odot$).

In this so-called Near-Surface Shear Layer (NSSL) the angular frequency $\Omega/2\pi$ increases inward by about 10–20 nHz (Miesch & Hindman 2011). Its nature is one of the puzzles being actively investigated nowadays (see Hanasoge et al. 2015 and references therein). Intriguingly, the depth of the NSSL is roughly equal to the characteristic size of supergranules observed at the photosphere, which is suggestive of some link between the supergranules and the depth of the surface shear layer (Hathaway 2011).

A plausible theory is that the structure of the NSSL is the outcome of a complex nonlinear coupling between the differential rotation and the MC (gyroscopic pumping), which involves a balance between small scale turbulent transport, large-scale mean flows, and a link to the deep CZ (Miesch & Hindman 2011).

In this mechanism, a minimum viscous dissipation is required to reproduce a realistic shallow meridional flow. A more recent theoretical work extending the global convection simulation to 0.99 $R_\odot$ proposes that the turbulent viscous stress that results from the radial gradient of the meridional flow is a driving mechanism for the maintenance of the NSSL (Hotta et al. 2015). On the other hand, ring-diagram based helioseismology measurements have very recently yielded pretty high values of the convective flow speeds in the subsurface of the NSSL. Horizontal flow velocities are seen to peak at 430 m $s^{-1}$ (rms) near the surface, decreasing to about 120 m $s^{-1}$ between 20 and 30 Mm at the bottom of the NSSL in contrast with previous measurements indicating an rms upper limit of 1 m $s^{-1}$ at a depth of 30 Mm (Greer et al. 2015). The newly measured amplitudes of the convective flow velocity in the NSSL give Rossby numbers 'Ro' above unity suggesting that convection in the NSSL is not significantly affected by the Sun's rotation ($\mathrm{Ro} = U/\Omega L$, where $U$ is a typical velocity amplitude, $\Omega$ is the rotation rate and $L$ is the characteristic length scale of convection).

Turbulent convection models generally assume that there is an important transfer of momentum in the Sun's CZ due to diffusion of the small-size turbulent eddies appearing as grain-like structures or granules on the surface with typical size $\sim$1 Mm across and fluctuating with typical vertical and horizontal velocities of 1–2 km $s^{-1}$. Molecular viscosity is then replaced in the conservation equations by a much larger *eddy* viscosity that can be estimated as $\nu_\mathrm{e} \sim u_\mathrm{e} l_\mathrm{e}$, where $u_\mathrm{e}$ is the typical eddy velocity and $l_\mathrm{e}$ is its size (Gilman 1979; Sturrock 1985; Stothers 2000). By using an eddy viscosity $\nu_\mathrm{e} \sim 10^9$ $\mathrm{m}^2$ $\mathrm{s}^{-1}$, negligible values of the *nominal* Prandtl number in stellar CZs of $10^{-6}$ – $10^{-10}$ instead become of the order of 1 – $10^{-2}$ (Sturrock 1985; Featherstone & Miesch 2015). Thus, viscous dissipation of momentum could become a phenomenon of similar importance to thermal transport. High-resolution nonmagnetic simulations of turbulent convection using the anelastic spherical harmonic (ASH) code have provided some insight into the processes that drive and shape the MC within the CZ (Miesch et al. 2008; Featherstone & Miesch 2015). The simulation solves the 3D equations of fluid motion in a rotating spherical shell under the anelastic approximation. The system domain extends from near the base of the CZ ($r = 0.71 - 0.72\ R_\odot$) to $r = 0.965 - 0.98\ R_\odot$.

Featherstone and Miesch (Featherstone & Miesch 2015) have conducted a sensitive analysis on the effects of the eddy kinematic viscosity and the thermal diffusivity ($\alpha_\mathrm{e}$) in the ranges $\nu_\mathrm{e} \sim 2 - 8 \times 10^9$ $\mathrm{m}^2$ $\mathrm{s}^{-1}$ and $\alpha_\mathrm{e} \sim 16 - 32 \times 10^9$ $\mathrm{m}^2$ $\mathrm{s}^{-1}$ at the surface, both decreasing with density as $\sim \rho^{-1/2}$ while the Prandtl number $\mathrm{Pr} = \nu_\mathrm{e}/\alpha_\mathrm{e} \sim 0.1 - 0.5$ was kept constant with depth. In a previous work (Miesch et al. 2008), they were fixed at $\nu_\mathrm{e} = 1.2{\times}10^8$ $\mathrm{m}^2$ $\mathrm{s}^{-1}$ and $\alpha_\mathrm{e} = 4.8{\times}10^8$ $\mathrm{m}^2$ $\mathrm{s}^{-1}$ throughout the computational domain, yielding a Prandtl number $\mathrm{Pr} = 0.25$. The simulations show a correlation between the MC and differential rotation as driven by the convective angular momentum transport. However, this link is thought to be quite sensitive to the subtle dynamics in the upper and lower boundary layers, which may significantly influence the MC profile in the solar CZ. Since the upper boundary (14 Mm below the photosphere) cannot be treated by the anelastic approximation, the possible influence of granulation and supergranulation on the MC near the photosphere cannot be resolved (Miesch et al. 2008).

Arguably, the shallow return of the MC currents inferred from recent observations could be due to a boundary layer effect that remains to be investigated (Featherstone & Miesch 2015). An important attribute of the anelastic approximation is that it removes pressure waves, which are filtered out by neglecting the $\partial\rho/\partial t$ term in the mass conservation equation. This can be justified only if the Mach number (Ma = convective fluid velocity/local sound speed) is very small for the turn-over time to be much longer than the acoustic time. If the fluid velocity is comparable to the local sound speed, a fully compressible model including acoustic waves is needed. The characteristic velocity of solar interior convective motions is indeed much smaller than the speed of sound with a Mach number on the order of $\mathrm{Ma} = 10^{-2}$. Yet, turbulent convection near the surface is intense and the Mach number may become close to unity (Christensen-Dalsgaard 2002). The possible correlation between turbulent convection and the Sun's acoustic oscillations is thus unknown. Some attempts to model oscillations in this thin layer have been made but the treatment of perturbations to the convective flux and turbulent pressure is not satisfactory (Christensen-Dalsgaard 2002). On the other hand, numerical simulations using Pencil Code have led also to interesting results regarding the cyclic magnetic activity due to turbulent convection (Käpylä et al. 2012; Karak et al. 2015). Remarkably, since these simulations allow for compressible flows, they could be useful to tackle the anelastic approximation limitation when the convective velocity is comparable to the sound speed.

## 2 ACOUSTIC STREAMING

Let us consider a standing pressure wave with finite wavelength $\lambda = 2\pi/k$ oscillating in a viscous fluid otherwise at repose and adjacent to a solid wall ($z = 0$ plane). The velocity of the fluid far from the boundary is

$$v_x = U_\mathrm{ex}\, e^{i\omega t},$$

where $U_\mathrm{ex}(x) = u_1 \cos(k\, x)$, $x$ is the direction of wave propagation, $u_1$ is the wave velocity amplitude, $\omega = 2\pi f$ and the non-slip and impenetrable boundary conditions ($v_x = v_z = 0$ at $z = 0$) apply. A perturbation analysis of the Navier-Stokes conservation equations yields a 2nd order time-independent circulation of the fluid near the wall of characteristic size $(\lambda/4) \times 1.9\delta_\nu$, where $\delta_\nu \sim \sqrt{\nu/\omega}$ is the distance of penetration of the rotational flow from the wall into the fluid (the so-called Stokes boundary layer) (Lighthill 1978). The streaming velocity at the edge of the Stokes boundary layer is given by Lighthill (1978)

$$u_\mathrm{s} = -\frac{3}{4}\frac{1}{\omega} U_\mathrm{ex} \frac{dU_\mathrm{ex}}{dx}, \tag{1}$$

with a maximum value

$$u_{\mathrm{s}} = \frac{3}{8}\frac{u_1^2}{c}, \tag{2}$$

where $c$ is the pressure wave speed. Remarkably, $u_{\mathrm{s}}$ is independent of the fluid viscosity despite being generated by viscous Reynolds-like stresses. It must be noted that Equation (1) yields the time averaged velocity of any particular parcel of the fluid (the Lagrangian mean flow), which serves to draw the fluid streamlines as experimentally tracked (i.e. what we see as the trajectory of a fluid parcel). The time-averaged Lagrangian velocity differs from the Eulerian velocity (the velocity of the fluid parcel that is present at a fixed position at a given instant) whose time-average is zero (Valverde 2015). The difference between the Lagrangian and Eulerian velocities is more generally known as Stokes drift. A similar scaling law to Equation (2) is obtained for the Stokes drift velocity ($u_{\mathrm{st}} \simeq u_1^2/2c$) induced by a surface gravity wave in a liquid.

Near boundary streaming (Schlichting or inner streaming) gives rise to a recirculation of the fluid outside the boundary layer (Rayleigh or outer streaming), which is determined by the system size and the slip velocity at the edge of the Stokes boundary layer (Lee & Wang 1990; Trinh & Robey 1994). In the case of a sound wave that impinges upon a circular cylinder whose radius is much smaller than the wavelength ($R \ll \lambda$) and in the limit of small oscillations with amplitude ($\xi_1/R \ll 1$) (Riley 1966; Gopinath & Mills 1993), the tangential component of the wave velocity is given by $U_{\mathrm{ex}} \approx 2v_1 \sin\theta = 2u_1 \sin(x/R)$, where $\theta$ is the polar angle and $x = R\theta$. Thus, the mean slip velocity is obtained as

$$u_{\mathrm{s}} = -\frac{3}{2}\left(\frac{u_1^2}{\omega R}\right). \tag{3}$$

In the case of a sphere a similar law can be derived ($u_{\mathrm{s}} \sim u_1^2/\omega R$).

For a spherical surface of radius $R$ and in the limit of small oscillations ($\xi_1 \ll R$)) the steady streaming motion takes the form of a hemispherically symmetric recirculation.

Figure 1a shows a schematic representation of the inner and outer streaming cells developed around a solid sphere immersed in a viscous fluid and subjected to a sound wave (or, equivalently undergoing translational oscillations in the viscous fluid). As may be seen, the fluid in the outer boundary circulates from the equatorial plane of symmetry toward both the upper and lower poles.

Acoustic streaming circulation patterns are usually observed in systems having in common the oscillations of a viscous fluid in the proximity of an interface (Valverde 2015).

Figure 1b shows the steady circulation patterns observed within a resonant tube. The transduction by mammalian inner ear hair is thought to be affected by acoustic streaming, which arises from cochlear traveling waves propagating in the liquid-filled inner ear (Lighthill 1992). Acoustic streaming occurs also in the protoplasm within individual cells of plant leaves, where steady circulation currents are induced by oscillations (Nyborg 1953). Another example is the vitreous humour in the eye, which exhibits a steady MC caused by the torsional oscillations of the eyeball (Repetto et al. 2008) (see Fig. 1c). Acoustic streaming is also observed within a pulsating liquid droplet (Mugele et al. 2011) as seen in Figure 2. MC is generated inside the liquid drop with a characteristic velocity $u_{\mathrm{s}}$ that conforms to Equation (2) (Mugele et al. 2011).

## 3 ACOUSTIC STREAMING AND MC IN THE SUN

A yet unexplored mechanism in solar physics is whether acoustic streaming arising from pressure oscillations in the Sun plays a relevant role on the MC observed in the CZ. To this end, it is necessary to quantify the relative strength of the characteristic streaming velocity that would result as compared to observed velocities and predicted by models based on the coupling between differential rotation and turbulent convection ($u_{\mathrm{s}} \sim 10 - 20$ m s$^{-1}$) (Featherstone & Miesch 2015). Obviously, the treatment of acoustic streaming in the Sun is much more complex than the study of a homogenous viscous fluid radially oscillating at a single frequency. The oscillation regime of the Sun is far more complicated and the amplitude of each one of the oscillation modes in the Sun is rather low ($\lesssim 0.1$ m s$^{-1}$) as experimentally observed and determined by the balance between the excitation rate and the damping rate from the stochastic turbulent excitation model (Houdek et al. 1999; Christensen-Dalsgaard 2002; Belkacem et al. 2008). The simultaneous excitation of millions of oscillation modes causes radial oscillations of the Sun's surface with amplitudes of hundreds of kilometers at frequencies mostly in the 2–4 mHz range (Christensen-Dalsgaard 2002; Belkacem et al. 2008). On the other hand, the turbulent viscosity in the CZ is decreased with density whereas pressure waves are progressively refracted as they propagate downward by the increase of temperature and depending on their wavelength (Christensen-Dalsgaard 2002). Clearly, an exhaustive analysis on the streaming flow associated with the simultaneous action of so many oscillation modes in such a complex fluid would require a full numerical study, which is outside the scope of this manuscript. In order to get a grip on the relevance of acoustic streaming we would assume then at the Sun's surface oscillates with a single frequency of $f \sim 3$ mHz and amplitude $\xi_1 = 100$ km, which gives an oscillation amplitude of $u_1 = 1.9$ km s$^{-1}$ (similar to the typical velocity of microturbulence at the Sun's photosphere, which is in the range 1–2 km s$^{-1}$). Using Equation (2) and $c \sim 100$ km s$^{-1}$ as a typical value of the sound speed near the photosphere we obtain $u_{\mathrm{s}} \simeq 10$ m s$^{-1}$ for the streaming velocity near the surface, which remarkably fits in the range of velocities reported for the near surface MC in the CZ of the Sun (Hathaway 2011; Hathaway et al. 2013; Featherstone & Miesch 2015). Note also that the stream-

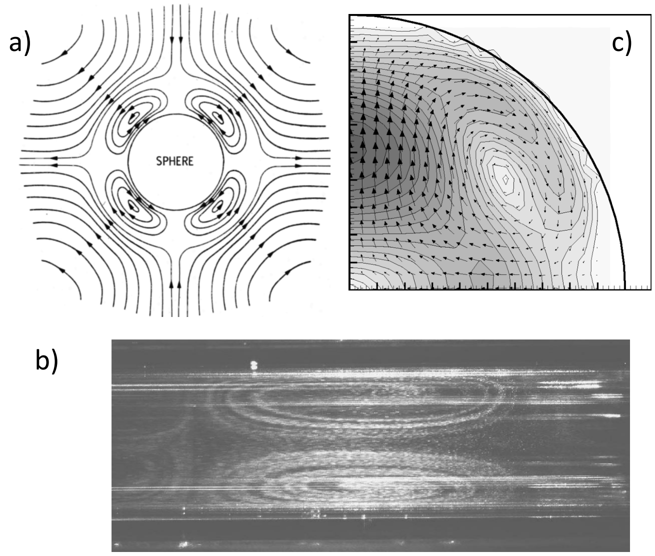


**Fig. 1** (a) Schematic representation of the steady circulation of fluid around a sphere in a standing acoustic wave in the horizontal direction or a sphere undergoing translational oscillations in the fluid otherwise at rest (reproduced from Leung & Wang 1985). (b) Acoustic streaming inside a resonant tube as visualized by particle image velocimetry (PIV) (reproduced from Campbell et al. 2000). (c) PIV visualization of the steady streaming flow of glycerol filling a spherical cavity undergoing periodic torsional oscillations around its vertical axis (reproduced from Repetto et al. 2008).

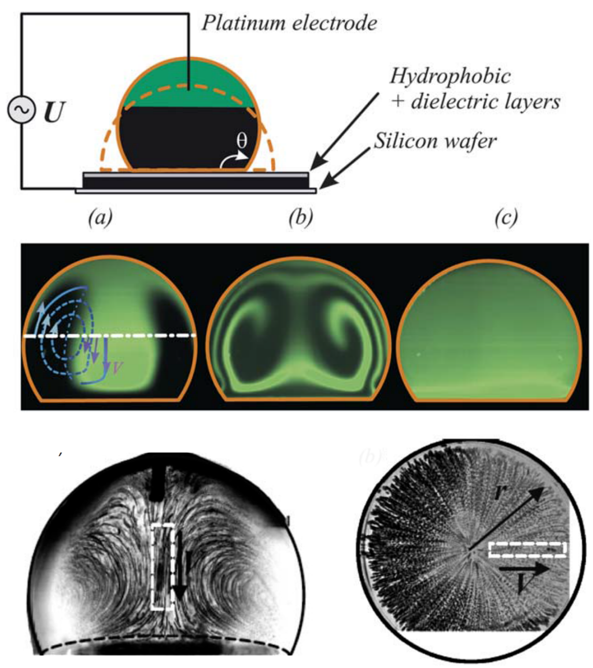


**Fig. 2** *Top*: Schematic representation of a liquid drop undergoing pulsations driven by an alternating applied voltage ($f = 120$ Hz). The snapshots show different states during oscillation. Lines in (a) sketch the steady streaming flow field that developed within the droplet. *Bottom*: vertical and horizontal cross-sections of the oscillating liquid drop showing steady large-scale streaming as traced by PIV of colloidal seed particles (reproduced from Mugele et al. 2011).

line pattern observed for a pulsating liquid drop (Fig. 2) resembles the MC in the CZ, although the oscillation pattern on the surface of the Sun is much more complicated. It may be thus argued that the study of acoustic streaming in the CZ of the Sun as affected by the radial surface oscillations deserves further analysis. An additional possibility is that acoustic streaming is developed by viscous dissipation of the waves refracted at the NSSL and radiative zone boundaries, which could in principle give rise to an MC near these boundaries of the type obtained for the refraction of an acoustic wave on a sphere (Fig. 1a). In this case however, it is difficult to obtain a simple estimation of the characteristic streaming velocity from Equation (2) that will depend on the combined action of the particular set of modes refracted in each surface, their frequency and amplitude. Moreover, in the boundary layers of the Sun, the limit $R \ll \lambda$ does not apply.

Acoustic streaming is used in applications for the enhancement of heat and mass transfer to intensify diverse processes (Yavuzkurt et al. 1991; Valverde 2015). The convective heat transfer as due to acoustic streaming has been analyzed theoretically by Gopinath and Mills (Gopinath & Mills 1993). The time averaged Nusselt number is determined by the Prandtl number 'Pr' and the streaming Reynolds number $\mathrm{Re_s}$ (defined as $\mathrm{Re_s} \equiv u_\mathrm{s} R/\nu$, where $R$ is a typical size of the system) according to the law

$$\mathrm{Nu} = \Lambda \mathrm{Re_s}^m \mathrm{Pr}^n, \tag{4}$$

where $m \simeq 0.5$. The prefactor $\Lambda$ and the exponent $n$ depend only slightly on the value of 'Pr'. Thus, $\Lambda \simeq 1$ and $n \simeq 0.5$ for Pr$<1$. The validity of Equation (4) is upheld by experimental measurements (Yavuzkurt et al. 1991; Gopinath & Harder 2000; Riley 2001). Typically, Nu varies in a range from $\mathrm{Nu} \sim 1$ (in the case of slow laminar flows) to $\mathrm{Nu} \sim 10^2 - 10^3$ in the case of intense convective flows. Using $u_\mathrm{s} \sim 10$ m s$^{-1}$, $R \sim R_\odot$ and $\nu = \nu_\mathrm{e} \sim 10^9$ m$^2$ s$^{-1}$, it is $\mathrm{Re_s} \sim 10$ and Nu$\sim 1$ for $\mathrm{Pr} \sim 0.1$, which implies that the contribution of acoustic streaming to the heat transport in the CZ would not be significant compared to turbulent convection.

An additional point that deserves further discussion is the parallelism existing between one of the mechanisms proposed for the excitation of pressure oscillations in the turbulent convective region of the Sun (thermal overstability) (Sturrock 1985; Houdek et al. 1999) and the amplification of acoustic waves in thermoacoutic engines (Swift 2002). Thermal overstability (Houdek et al. 1999) and stochastic excitation by turbulent convection (Belkacem et al. 2008) are considered the most plausible mechanisms for the excitation of pressure waves in the CZ. *Thermal overstability* operates if large enough temperature gradients exist capable of amplifying the oscillations of fluid parcels.

As the gas parcels move back and forth in each oscillation cycle (compressing and expanding, respectively) a net work is added to the acoustic wave if the temperature change in the surroundings is higher than the variation of temperature suffered by the fluid parcel due to adiabatic compression and expansion. The thermodynamic cycle of a fluid parcel in the CZ would thus resemble that of a fluid parcel in a thermoacoustic engine. In their most simplified version, thermoacoustic engines basically consist of a resonant tube filled with a viscous fluid in which a standing acoustic wave is subjected to a gradient of temperature (Swift 2002). The fluid parcels interchange heat with the walls as they compress and expand adiabatically. Work is added to the fluid parcel if there is a sufficiently large temperature gradient across the resonant tube similar to what happens in the thermal overstability mechanism in the Sun. The amplification of the sound wave leads to a perturbation of the characteristic streaming velocity, which might also occur in the Sun if thermal overstability operates. By assuming that acoustic oscillations are small (to justify a linearization of the Navier-Stokes equations) and that the core of the flow within the resonant tube was inviscid, the characteristic streaming velocity in a thermoacoustic engine is given by Rott (1974),

$$\begin{aligned} u_\mathrm{s} &= -\frac{3}{4}\frac{1}{\omega} U_\mathrm{ex} \frac{dU_\mathrm{ex}}{dx}(1+c_1) \\ &\quad + c_2 \frac{U_\mathrm{ex}^2}{2\omega}\frac{1}{T_m}\frac{dT_m}{dx}, \end{aligned} \tag{5}$$

where

$$c_1 = \frac{2}{3}(1-\varsigma)(\gamma-1)\frac{\sqrt{\mathrm{Pr}}}{1+\mathrm{Pr}}, \tag{6}$$

$$c_2 = \frac{(1-\varsigma)(1-\sqrt{\mathrm{Pr}})}{2(1+\sqrt{\mathrm{Pr}})(1+\mathrm{Pr})}. \tag{7}$$

Here, $\varsigma$ is the exponent in the assumed power-law dependence of viscosity on temperature ($\nu \sim T^{(1+\varsigma)}$) and $\gamma$ is the isentropic expansion factor of the gas (adiabatic index). Because the gas in the Sun behaves nearly like an ideal gas, these are $\gamma \simeq 1.6$ and $T \propto \rho$ (Featherstone & Miesch 2015). On the other hand, since kinematic viscosity in the CZ decreases with density according to the law $\nu_\mathrm{e} \propto \rho^{-1/2}$ (Featherstone & Miesch 2015), the exponent is $\varsigma = -3/2$, which contrasts with the increase of (molecular) viscosity with temperature for common gases. Using $\mathrm{Pr} = 0.1$ as a typical value (independent of density) (Featherstone & Miesch 2015) gives values of $c_1 = 0.3$ and $c_2 = 0.6$. Thus, the correction factor on the characteristic streaming velocity will be significant only for very high local temperature gradients. In the case of thermally driven acoustic oscillations in a thermoacoustic engine, the second term is not small, which gives rise to an important drift near the resonant tube wall and towards the hot end (Rott 1974). A further possibility to be explored in a more detailed analysis of MHD conservation equations is whether a steady flow due to acoustic streaming could be modulated by the magnetic field. Global convection simulations suggest the existence of a time varying circulation (Karak et al. 2015), which can have a profound effect on variations of the solar cycle according to some dynamo models (Karak 2010; Karak & Choudhuri 2013).

## 4 CONCLUSIONS

Acoustic streaming is a universal phenomenon that occurs whenever a bounded viscous fluid oscillates. The main feature of acoustic streaming is the development of a steady rotational flow of the viscous fluid near the interface (inner streaming). Inner streaming drives in turn the onset of a steady circulation of fluid outside the boundary layer (outer streaming) whose strength is decreased with the distance to the boundary. Acoustic streaming in spherical boundaries usually assumes an MC pattern closely resembling the MC observed in the CZ.

In this manuscript, it is argued that acoustic oscillations of the Sun might lead to this type of streaming in the CZ, quite similar to the steady streaming that develops within a pulsating droplet of a viscous fluid. A simple estimation of the associated drift velocity yields $u_\mathrm{s} \sim 10$ m s$^{-1}$ of the same order of the observed MC velocities in the Sun. A rigorous numerical analysis should consider the interaction of pressure waves and turbulent convection usually neglected as well as the refraction of pressure waves in the boundary layers of the CZ that might also give rise to steady streaming currents. Acoustic streaming is present in a vast number of natural systems and scales. It happens in our eye and ear, plant cells, pulsating flows (think about the flow of blood through veins and arteries), vibrating structures and fluids, etc. The perspective that it might also be occurring in the Sun is certainly appealing.

**Acknowledgements** Financial supports by the Andalusian Regional Government (Junta de Andalucia, contract FQM-5735) and Spanish Government Agency Ministerio de Ciencia e Innovacion (contract CTQ2014-52763-C2-2-R) are acknowledged.

## References

Arkhypov, O. V., Antonov, O. V., & Khodachenko, M. L. 2012, Sol. Phys., 278, 285
Belkacem, K., Samadi, R., Goupil, M.-J., & Dupret, M.-A. 2008, A&A, 478, 163
Campbell, M., Cosgrove, J. A., Greated, C. A., Jack, S., & Rockliff, D. 2000, Optics Laser Technology, 32, 629
Choudhuri, A. R., Schussler, M., & Dikpati, M. 1995, A&A, 303, L29
Christensen-Dalsgaard, J. 2002, Reviews of Modern Physics, 74, 1073
Featherstone, N. A., & Miesch, M. S. 2015, ApJ, 804, 67
Gilman, P. A. 1979, ApJ, 231, 284
Gopinath, A., & Harder, D. R. 2000, International Journal of Heat and Mass Transfer, 43, 505
Gopinath, A., & Mills, A. F. 1993, The Journal of the Acoustical Society of America, 94, 1773
Greer, B. J., Hindman, B. W., Featherstone, N. A., & Toomre, J. 2015, ApJ, 803, L17
Hanasoge, S., Miesch, M. S., Roth, M., et al. 2015, Space Sci. Rev., 196, 79
Hathaway, D. H. 2011, arXiv:1103.1561
Hathaway, D. H., Upton, L., & Colegrove, O. 2013, Science, 342, 1217
Hazra, G., Karak, B. B., & Choudhuri, A. R. 2014, ApJ, 782, 93
Hotta, H., Rempel, M., & Yokoyama, T. 2015, ApJ, 798, 51
Houdek, G., Balmforth, N. J., Christensen-Dalsgaard, J., & Gough, D. O. 1999, A&A, 351, 582
Käpylä, P. J., Mantere, M. J., & Brandenburg, A. 2012, ApJ, 755, L22
Karak, B. B. 2010, ApJ, 724, 1021
Karak, B. B., & Choudhuri, A. R. 2013, RAA (Research in Astronomy and Astrophysics), 13, 1339
Karak, B. B., Jiang, J., Miesch, M. S., Charbonneau, P., & Choudhuri, A. R. 2014, Space Sci. Rev., 186, 561
Karak, B. B., Käpylä, P. J., Käpylä, M. J., et al. 2015, A&A, 576, A26
Lee, C. P., & Wang, T. G. 1990, The Journal of the Acoustical Society of America, 88, 2367
Leung, E. W., & Wang, T. G. 1985, Acoustical Society of America Journal, 77, 1686
Lighthill, J. 1978, Waves in fluids (Cambridge: Cambridge Univ. Press)
Lighthill, J. 1992, Journal of Fluid Mechanics, 239, 551
Lord, J. W., Cameron, R. H., Rast, M. P., Rempel, M., & Roudier, T. 2014, ApJ, 793, 24
Miesch, M. S., Brun, A. S., DeRosa, M. L., & Toomre, J. 2008, ApJ, 673, 557
Miesch, M. S., & Hindman, B. W. 2011, ApJ, 743, 79
Mugele, F., Staicu, A., Bakker, R., & van den Ende, D. 2011, Lab on a Chip, 11, 2011
Nyborg, W. L. 1953, Acoustical Society of America Journal, 25, 68
Pipin, V. V., & Kosovichev, A. G. 2013, ApJ, 776, 36
Repetto, R., Siggers, J. H., & Stocchino, A. 2008, Journal of Fluid Mechanics, 608, 71
Riley, N. 1966, The Quarterly Journal of Mechanics and Applied Mathematics, 19, 461
Riley, N. 2001, Annual Review of Fluid Mechanics, 33, 43
Rott, N. 1974, Zeitschrift Angewandte Mathematik und Physik, 25, 417
Roudier, T., Švanda, M., Rieutord, M., et al. 2014, A&A, 567, A138
Stothers, R. B. 2000, MNRAS, 314, L7
Sturrock, P. A. 1985, Physics of the Sun: Volume II: The Solar Atmosphere, Geophysics and Astrophysics Monographs: An International Series of Fundamental Textbooks (Springer Science & Business Media)
Swift, G. W. 2002, Thermoacoustics: A Unifying Perspective for Some Engines and Refrigerators (Acoustical Society of America)
Trinh, E. H., & Robey, J. L. 1994, Physics of Fluids, 6, 3567
Valverde, J. M. 2015, Contemporary Physics, 56, 338
Yavuzkurt, S., Ha, M., Reethof, G., Koopmann, G., & Scaroni, A. 1991, Journal of Energy Resources Technology, 113, 286